ASSOCIATION
OF SCIENTISTS
AND ENGINEERS

MK 66 ROCKET SIGNATURE REDUCTION

JAMES D. HABERSAT

19TH ANNUAL TECHNICAL SYMPOSIUM 1982

ASSOCIATION OF SCIENTISTS AND ENGINEERS OF
THE NAVAL SEA SYSTEMS COMMAND
DEPARTMENT OF THE NAVY – WASHINGTON, D.C. 20360

(2)

MK 66 ROCKET SIGNATURE REDUCTION

James D. Habersat

Physicist

Naval Ordnance Station

Indian Head, Maryland

April 1982

Approved for Public Release

Distribution Unlimited

The views expressed herein on the personal opinions of the author and are not necessarily the official views of the Department of Defense or of the Department of the Navy

ABSTRACT

A limited signature reduction study for the 2.75-inch rocket was conducted at the Naval Ordnance Station (NAVORDSTA), Indian Head, Maryland. The objective of the study was to reduce the visible signature of the rocket motor.

The rocket motor used for demonstration tests was the MK 66, which burns for approximately one second. It contains a double-base, non-aluminized propellant. The visible signature is primarily smokeless, consisting mainly of a bright orange flame resulting from afterburning of the fuel-rich exhaust.

The technical approach consisted of incorporating additional potassium sulfate (K_2SO_4) with an ablative binder into internal rocket motor components. During motor firing, erosion of the binder released K_2SO_4 into the combustion gases. The resulting potassium ions served to inhibit secondary combustion in the exhaust plume.

Modified motors were static fired and afterburning results compared to those for an unmodified MK 66 motor firing. For the modified motors, there was no visible signature over the first half (0-0.5 seconds) of the motor burn time. This is a significant improvement over the nominally 0.1 second flashless interval for the unmodified motor.

TABLE OF CONTENTS

INTRODUCTION

The purpose of this study was to investigate a proposed method of suppression of the visible plume of the MK 66 Rocket. Suppression of the visible signature would significantly improve helicopter pilot vision during night-time mission operations, and also serve to reduce launch platform vulnerability. This potential improvement involved incorporating additional potassium sulfate (K_2SO_4) into the motor resonance/salt rod, and replacing the standard propellant grain end sleeve with one containing a quantity of K_2SO_4. Ablation of the salt rod and end sleeve during firing releases K_2SO_4 into the rocket exhaust. The K_2SO_4 acts to inhibit combustion of the fuel-rich exhaust when it mixes with atmospheric oxygen.

AFTERBURNING

The combustion of exhaust products with the air entrained in the plume is called afterburning. The afterburning creates atoms and molecules with excited internal states which, upon decay, emit radiation in the ultraviolet (UV), visible, and infrared (IR) portion of the spectrum. Afterburning, by raising the temperature of the rocket exhaust, can also serve to increase emissions, as defined by Plank's law for black body radiation.

Two basic methods are available for chemical suppression of afterburning: increasing oxidizer content of the propellant to achieve complete combustion of the fuel, and incorporating additives in the propellant itself or its exhaust stream which inhibit combustion in the plume. Usually, increasing oxidizer content is not a feasible approach, as both burning rate and propellant mechanical properties may be altered. Additives are commonly used in gun propellants for elimination of muzzle flash. Their use in tactical rockets has been very limited, and directed only at elimination of ignition flash for air-launched rockets.

Additives, used in small quantities, may be incorporated into the propellant or released (through ablation) into the exhaust stream. In gun propellants the additives are incorporated directly into the propellant, and the minute quantities used do not significantly alter the basic physical and chemical properties. K_2SO_4 has been found to be an effective additive for flame suppression.[1] A probable chemical mechanism is production of potassium hydroxide (KOH) in the exhaust, which suppresses combustion by reacting with hydrogen (H) and hydroxide (OH) radicals, producing potassium (K), potassium oxide (KO), and water (H_2O). The inhibition reactions are:

$$KOH + H \longrightarrow K + H_2O$$
$$KOH + OH \longrightarrow KO + H_2O$$

These reactions compete with the chain propagating reactions for the combustion of carbon monoxide (CO) and molecular hydrogen (H_2) with atmospheric oxygen (O_2):

$$CO + OH \rightarrow CO_2 + H$$
$$H + O_2 \rightarrow OH + O$$
$$O + H_2 \rightarrow OH + H$$
$$OH + H_2 \rightarrow H_2O + H$$

KOH is thus a scavenger of the active species H and/or OH radicals. CO and H_2 are the major fuels in the exhaust of a non-aluminized double base propellant.

The chemical suppression mechanisms serve to reduce plume temperatures for use of only a small amount of the additive. Above some threshold quantity the afterburning is extinguished, and additional additive is redundant.

FLAMEHOLDING

One of the peculiar features of the afterburning associated with the MK 66 rocket is that the visible flame is located some distance aft of the nozzle exit plane. This is due to the use of an under expanded nozzle which results in little or no mixing occuring until optimum expansion is reached outside and aft of the nozzle.

There are several mechanisms by which localized ignition may occur in the plume flow field.[2] These include shock heating, base recirculation, and separated flow. In a purely viscous plume model (which ignores shocks), the only mechanism present for ignition depends on having a sufficiently high temperature at the points in the plume where oxidizer (atmospheric O_2) and fuel (mainly CO and H_2) are in the proper proportions to react fast enough to burn and significantly raise the plume temperature. However, in the real rocket motor exhaust environment, shocks do exist (such as Mach diamonds) which create localized hot spots causing localized ignition for afterburning. Even when the pressure is reduced downstream, the flame holding action may continue due to increased gas temperature and increased free radical concentrations propagating from the flameholder position. Figure 1 depicts this motor exhaust environment in which flame holding may occur.

APPROACH

The objective of the test program was to eliminate or substantially reduce the visible signature of the MK 66 rocket. A decision was made early in the program to exclude the propellant from any changes. It was felt that hardware changes alone could accomplish the objective and be more cost effective. Success of the test program could then possibly result in a retrofit program of the MK 66 motor inventory.

The standard MK 66 rocket utilizes a resonance rod coated with K_2SO_4 in an ethyl cellulose (EC) binder. Flashless burning is observed for only the first 0.1 seconds of the nominal 1.0 second burn. It was postulated that by increasing the amount of K_2SO_4 available, this flashless burning time could be extended.

Attention was directed towards modifying the motor resonance rod and propellant grain end sleeve. Figure 2 shows the locations of these components in the motor.

The standard resonance rod consists of a salt cylinder bonded to a 0.156-inch diameter steel rod. The salt cylinder has a 0.331-inch diameter and a length of 17.0 inches. The formulation is a nominal 70% K_2SO_4 and 30% EC. The resonance rod has a dual function: control combustion instability, and control afterburning during and immediately after motor launch. The resonance rod is also referred to as the salt rod.

The MK 66 rocket normally has an EC end sleeve bonded to the aft end of the propellant grain. This end sleeve serves to insulate the forward portion of the nozzle from the hot exhaust gases.

The proposed modifications consisted of increasing the diameter of the salt cylinder on the resonance rod to 0.500 inches, and formulating the end sleeve from 50% K_2SO_4 and 50% EC.

To evaluate the proposed changes, a total of seven motors was fired on two different dates. The first set consisted of two standard MK 66 motors, and

two motors with the modified salt rod. The second set of firings consisted of one standard MK 66 motor, one motor with the standard salt rod and the salted end sleeve, and one motor with both a modified salt rod and a salted end sleeve. Table I summarizes the configurations fired.

The test set-up is shown in Figure 3. A Warner Swasey Rapid Scanning Spectrometer was used to measure visible light (400-700 nm) emissions. Camera coverage with daylight film included a 35mm single lens reflex camera, a 100 frames per second movie camera, and a 1000 frames per second movie camera. In addition, a Polaroid camera was used during firings for on-the-site feedback to verify proper camera aiming and exposure. The motors were instrumented to measure thrust and pressure.

Table I. Firing Matrix.

No.	Date	Configuration: Resonance (Salt) Rod	Configuration: End Sleeve
1	March 1979	Standard	Standard
2	March 1979	Standard	Standard
3	March 1979	Modified	Standard
4	March 1979	Modified	Standard
5	August 1979	Standard	Standard
6	August 1979	Standard	Modified
7	August 1979	Modified	Modified

RESULTS

A more comprehensive report of the test firings and results can be found in references 3 and 4. Pertinent data are summarized below.

K_2SO_4 ANALYSIS OF COMPONENTS

The salted end sleeve and salt rod were analyzed to verify salt content. The results of the analysis are shown in Table II. The data indicated that salt content was higher than expected. No adverse impact on the test firings was anticipated.

Table II. Salt Weight Percent

Component	% K_2SO_4
End Sleeve	56.5
Resonance (Salt) Rod	75.7

BALLISTIC PERFORMANCE

Ballistic performance results from the seven firings are shown in Table III. The nominal data represents a historical average for MK 66 motors produced at NAVORDSTA. The slightly low impulse and pressures of the test motors are characteristic of the propellant lots that were used. The presence of a salted end sleeve and/or modified salt rod in the motor had no noticeable effect on ballistic performance.

Table III. Ballistic Performance (70°F).

Motor No.	Ignition Delay (sec)	Ignition Pressure (psia)	Maximum Pressure (psia)	Action Time (sec)	Impulse (lbs-sec)
1	0.010	1670	1920	1.02	1499
2	0.010	1600	1860	1.05	1495
3	0.010	1700	1980	1.01	1482
4	0.010	1680	1940	1.02	1484
5	0.011	1619	1831	1.03	1466
6	0.012	1565	1669	1.12	1508
7	0.011	1657	1782	1.03	1515
nominal	0.016	1600	1772	1.09	1548

SPECTROMETER DATA

The firings were monitored using a Warner-Swasey spectrometer, gated to accept the visible spectrum (400 to 700 nm). The spectrometer produced 80 scans per second. Consecutive sets of 4 scans each were averaged together to obtain composite scans spaced at 0.05 second intervals (20 composite scans per second).

The composite scans were then adjusted to correct for the spectral sensitivity of the human eye. Human eye sensitivity varies as a function of wavelength. Figure 4 plots eye sensitivity of a standard observer at different wavelengths for normal levels of illumination. A curve fitting equation was generated to fit these data, and then applied to each composite scan to give an adjusted spectral radiance curve. The adjusted curve represents spectral radiance as it would be seen by the helicopter pilot.

One of the resulting composite scans is shown in Figure 5. The scan shown is for the standard MK 66 motor (motor No. 1) that was fired. The scan was recorded 0.52 seconds after ignition. The top curve represents the actual data, and the bottom curve is the adjusted data. Spectrometer radiance output was not calibrated, and the radiance scale is therefore in arbitrary units. Program software computed the area under each curve to determine apparent intensities for each time or scan.

It is apparent from Figure 5 that the blackbody radiation does not make a significant contribution to the MK 66 signature. Blackbody radiation occurs over a continuum. The data seen in Figure 5 contain peaks and valleys, characteristic of emission/absorption spectra of atomic and molecular species. Since the AA-2 propellant used in the MK 66 is non-metallized, this type of data is expected. The central peak in Figure 5 is probably due to atomic sodium (which has a doublet at 589 and 590 nm). Trace amounts of sodium were found to be present in both the salt rod and salted end sleeve. The other two peaks may be due to calcium, which has lines 554 and 622 nm.

The apparent intensities (areas under the curves) were plotted as a function of time for each motor. These plots were then combined, resulting in the data shown in Figures 6 and 7. Note that due to an equipment malfunction, no data are available after 0.57 seconds for the MK 66 motor containing both a large diameter salt rod and a salted end sleeve.

To assess the relative performance of the motors, the area under the curves of Figure 6-7 was determined. The 0.57 second time was used because of the equipment malfunction that occurred on the large diameter salt rod plus salted end sleeve motor. The percent signature reduction for the modified motors was then calculated, using the standard MK 66 motor as the baseline. Table IV presents these data.

Table IV. % Reduction of Visible Light

Motor Type	Visible Spectrum	% Reduction up to 0.57 sec	% Reduction full scale
Salted End Sleeve	Absolute	41	21
	Human Eye	48	31
Large Diameter Salt Rod	Absolute	53	37
	Human Eye	56	37
Salted End Sleeve and Large Diameter Salt Rod	Absolute	73	--
	Human Eye	83	--

Delay time from motor ignition to the start of afterburning can also be determined from Figures 6-7. The start of afterburning was arbitrarily defined as 10% of the maximum intensity achieved by the standard motor. These data are shown in Table V.

Table V. Afterburning Delay Times.

Motor Type	Delay Time (sec)
Standard	0.122
Salted End Sleeve	0.226
Large Diameter Salt Rod	0.245
Salted End Sleeve Large Diameter Salt Rod	0.418

HIGH SPEED CAMERA COVERAGE

The firings were also monitored by a high speed (1000 frames/second) motion picture camera. The time base used for the spectrometer coverage was simultaneously recorded on the film to enable valid cross reference. Film of the last three motors (nos. 5, 6 and 7) fired was studied. Frames of the movie film at points corresponding to 0.05 second intervals were analyzed. At each interval the apparent cross sectional area of the plume was determined, along with the distance behind the nozzle at which the afterburning started. These data are shown in Figures 8 and 9.

Although plume cross sectional area is not strictly proportional to plume intensity, it is a qualitative indicator. Figure 8 ranks the three test motors in the same order as the spectrometer data, and thus increases the credibility of Figures 6 and 7.

Figure 9 shows that the distance behind the motor at which afterburning starts is both dependent on motor type, and burn time.

POST TEST INSPECTION

After firing, all motors were downloaded and inspected to evaluate condition of the end sleeves and salt rods.

The inside diameters of both the normal end sleeves and the salted end sleeves were approximately the same. Before firing, the inside diameter of the end sleeve is 1.500 inches. After firing, the inside diameters ranged from 1.750 to 1.850 inches.

The overall length of the normal end sleeve and the salted end sleeves were different. Before firing, the overall length of the end sleeve is 0.925 inches. After firing, the length of the normal end sleeve varied between 0.825 and 0.870, while the salted end sleeve length varied from 0.490 to 0.755 inches.

The standard salt rods used also had a different appearance from the large diameter salt rod. The salt was completely gone from the resonance rods of the standard motors. The resonance rod with the large diameter salt had a cone of salt remaining on the rod at the most forward end of the salt's original location. The apex of the cone pointed towards the aft end of the motor. The base of the cone measured 0.387 inches (versus 0.500 inches before firing) and tapered out 6.4 inches aft along the rod, with the rod bare of salt aft of this point.

CONCLUSIONS

Program achievements are basically summarized in Figures 6-7 and Tables IV-V. The high speed camera coverage gives visual supportive data that affirms the spectrometer data.

Salted end sleeves and large diameter salt rods used alone, have approximately equal effectiveness in suppressing afterburning. When combined, the two components act together to give a 70% or greater reduction in visible flash over the first half of the motor burn time.

This marks a significant reduction in the visible flash associated with the standard MK 66.

Unfortunately, no data is available on the second half of burn time for the salted end sleeve plus large diameter salt rod combination. The program's limited funding resulted in only one sample of each motor type being assembled and fired. Thus the program was vulnerable to equipment failure.

Further firings of the salt rod, end sleeve combination are needed to fully characterize the motor, and build up a data base. Hot and cold firings should be undertaken to determine temperature dependence. Further improvements in signature reduction may also be possible through modification of other components.

REFERENCES

1. Edward T. McHale, "Suppression of Missile Plume Infrared Signature", Atlantic Research Corp., submitted to Naval Ordnance Station under contract N00174-74-C-0270, ARC Ref. No. 47-5626, dated 20 October 1975.

2. Rocket Exhaust Plume Technology, Chemical Propulsion Information Agency, Johns Hopkins University Applied Physics Laboratory, publication #263.

3. Naval Ordnance Station, Indian Head, Md., Internal Memorandum 5251:434:79, dated 10 May 1979. Subj: MK 66 Rocket Concept Verification Program for Signature reduction; final report.

4. Naval Ordnance Station, Indian Head, Md., Internal Memorandum 5251:512:79, dated 27 September 1979. Subj: MK 66 Rocket Signature Reduction; salted end sleeve evaluation firings.

FIGURES

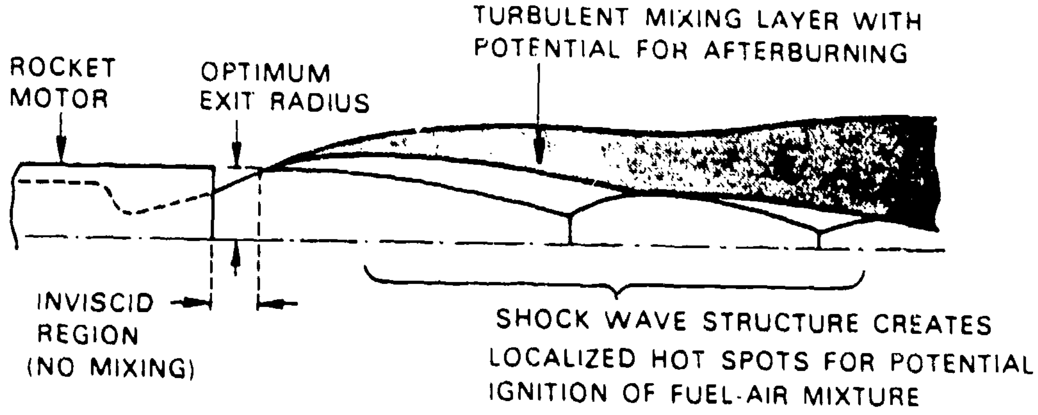

FIGURE 1. FLAME HOLDING

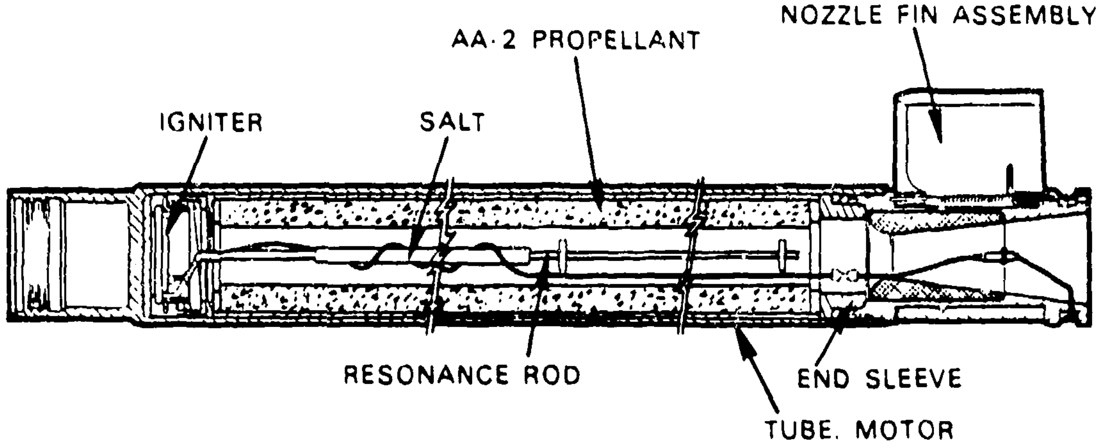

FIGURE 2. MK 66 MOTOR

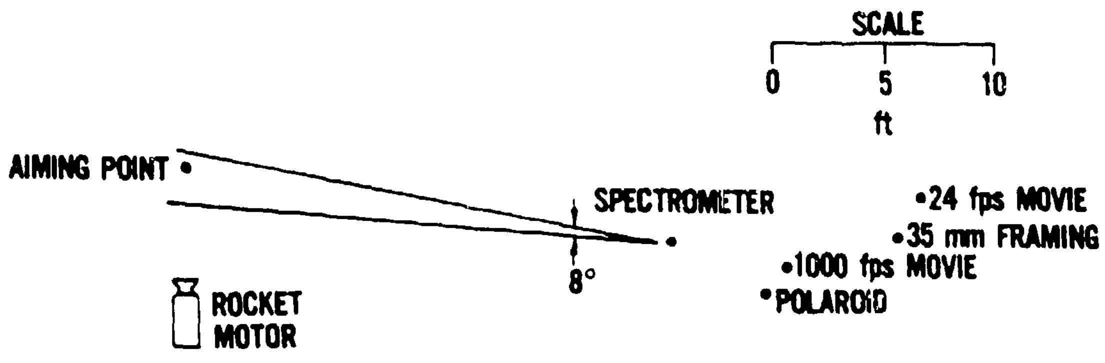

FIGURE 3. TEST SET-UP

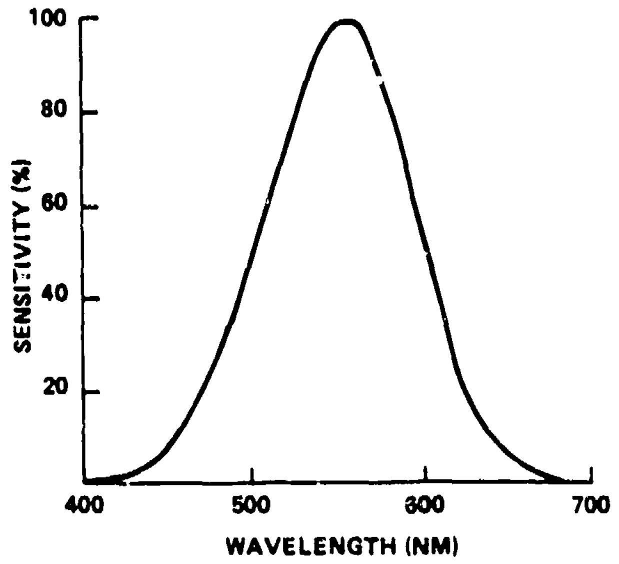

FIGURE 4. RELATIVE EYE SENSITIVITY

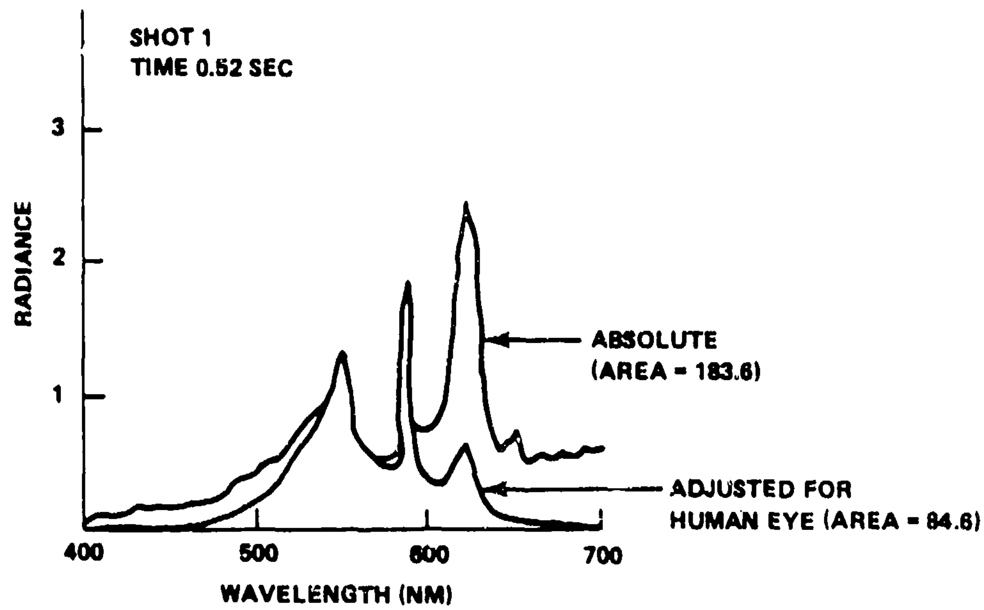

FIGURE 5. REPRESENTATIVE COMPOSITE SCAN

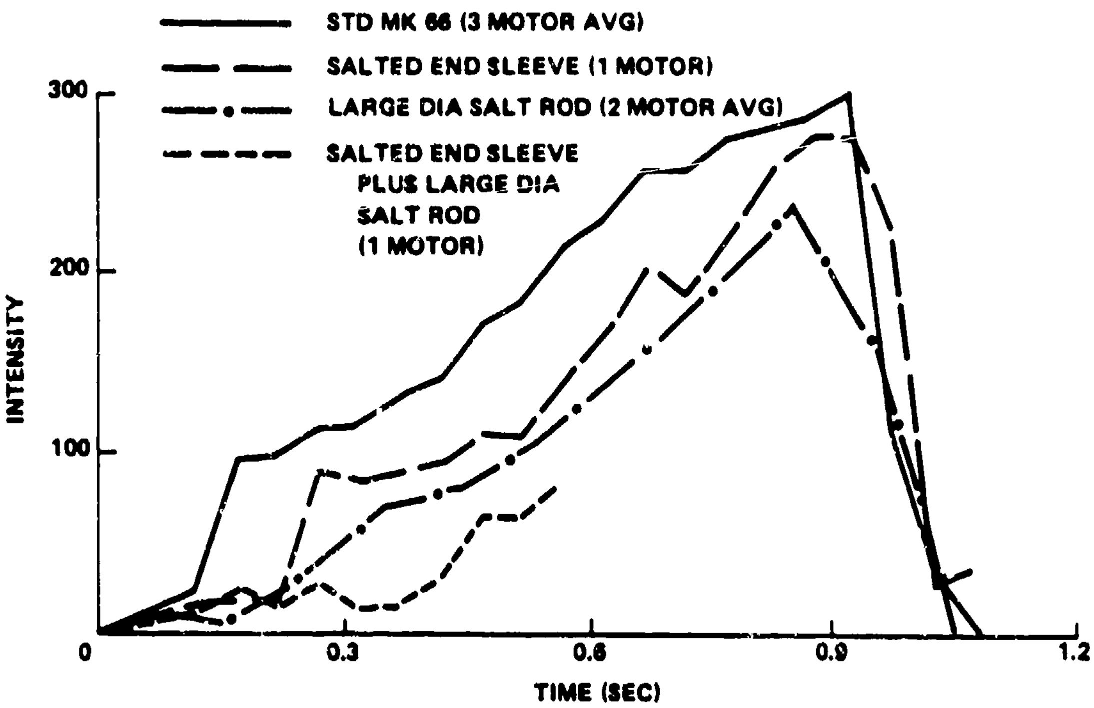

FIGURE 6. ACTUAL EMISSIONS

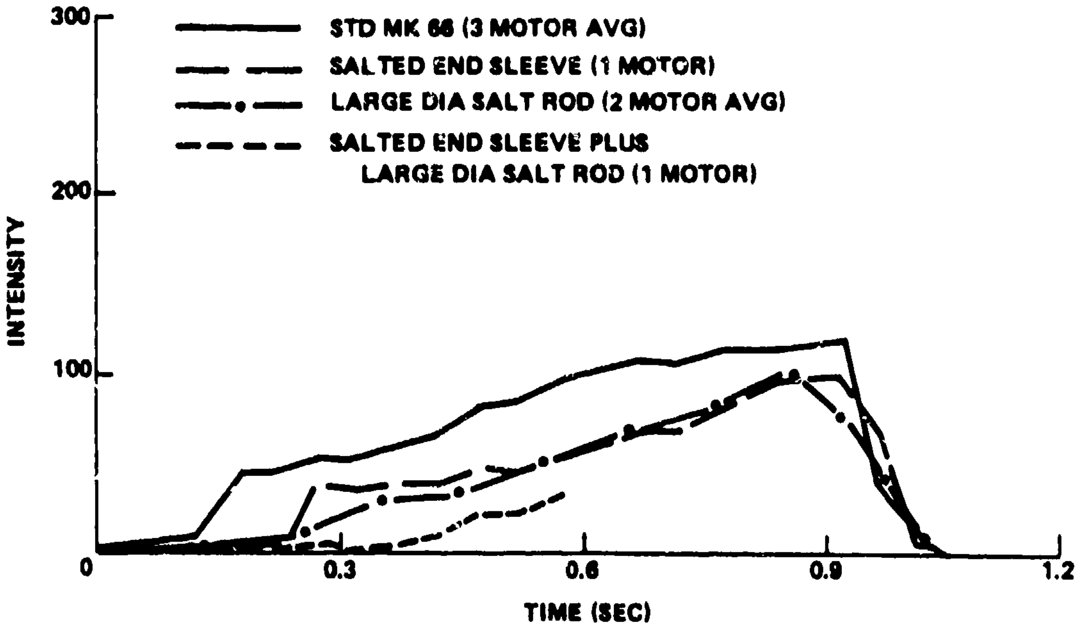

FIGURE 7. HUMAN EYE ADJUSTED EMISSIONS